한국해양공학회지 제17권 제1호, pp 26~32, 2003 (ISSN 1225-0767)

Wave Absorption Control for Torsional Vibration

DONG-HO NAM* AND MUNEHARU SAIGO**
*Dept. of Mechanical Design Engineering, Incheon City College, Incheon, Korea, Currently with AIST, Japan
**Smart Structure Research Center,
National Institute of Advanced Industrial Science and Technolgy (AIST), Tsukuba, Japan

KEY WORDS : Wave Absorption Control, Vibration Control, Torsional Vibration, Imaginary System, Initialization

ABSTRACT : *기존 대부분의 진동제어법이 모드제어에 근거한 것인데 반면, 본 연구에서는 진동억제의 또다른 방법인 파동제어기법을 다루었다. 무반사조건을 만족하면서 진동에너지를 흡수하는 파동제어는 특히 1차원 구조계에 유용하게 사용될 수 있으리라고 기대되는데, 현실적으론 제어알고리즘의 실현화에 그 어려움이 있다. 본 연구에서는 근사화된 무한구조계를 계산기내에 구축하여, 진동에너지가 근사 무한구조계에 흡수되는 조건을 제어기가 실현하는 제어수법을 개발하였다. 시뮬레이션과 실험을 통하여, 본 연구에서 제안한 파동제어기법에 의해 회전체의 비틀림 진동억제가 효율적으로 이루어짐을 확인할 수가 있었다.*

1. Introduction

Active vibration suppression in structures and mechanical systems consists primarily of the modal vibration control and wave-absorption control. Modal vibration control is based on natural vibration modes, i.e., the system's standing-wave state. Wave absorption control is based on vibration energy absorption by impedance matching, i.e., the system's progressive-wave state. Modal vibration control is used widely in different fields, but wave absorption control has advantages over modal vibration control in certain fields. The wave absorption process is conducted based on local wave propagation properties, with no need to deal with total system to control, and it is applicable to any system even if only information on the structure where waves propagate is known. Wave absorption control, however, requires information on where waves propagate, making it suitable for 1-dimensional (1D) structures or assemblies of 1D-elements. Wave control on 1D-structures has been widely studied. Von Flotow (1986a, 1986b) and Miller and Von Flotow(1989) treated truss structures and power flow, and Fujii et al.(1992a, 1992b) discussed design procedures for wave-absorption controllers with non-collocated sensors and actuators. Elliott and Billet(1993) studied controllers with adaptive digital filters for beams, and Gardonio and Elliott(1996) dealt with longitudinal and flexural waves in beams. Matsuda et al.(1998) discussed a FEM-based transfer matrix approach, and Utsumi(1999) presented analytical implementation of wave absorption control for beams.

제1저자 남동호 연락처 : Tsukuba Central 2, Ibaraki, Japan
+81-90-5316-4887 dh.nam@aist.go.jp

The above studies dealt with continuous structures such as beams and truss structures. Wave propagation in periodic structures of lumped systems has long been treated(Brillouin, 1946), but wave absorption control research on lumped systems has been less so. Examples include O'ccoure's(1998) treatment of a lumped parameter mass-and-spring system as a model of a flexible arm and Saigo et al.'s(1998) study of a multiple-pendulum system. Another problem of wave absorption control is that the control law includes the square root of Laplacian s, which cannot be implemented in real hardware by usual methods, meaning most studies in experiments have used approximations of the control law. To overcome this problem, we present a new method(Saigo et al., 1998) that uses online computer simulation of a large degree-of-freedom (DOF) structural system having properties similar to the actual controlled system. This "imaginary" system is connected virtually to the real system by an actuator satisfying the continuity condition between real and imaginary systems, which we term wave-absorption control with an imaginary system (WCIS). WCIS realizes an infinite structural system free of wave reflections in the controlled real system if a suitable process is conducted to clear the vibrating energy in the imaginary system at appropriate timing. For this, WCIS initializes the imaginary system where deflections and velocities of all elements are set to zero except for the end element of the connecting side. Initialization should be done before the reflecting wave from the end of the imaginary system reaches the real system. In a previous study(Saigo et al., 1998), we applied WCIS to free vibrations where total vibration energy is limited. It is not clear at this stage if WCIS is applicable to a general mechanical vibration system such as the mode-based vibration control strategy.

We apply WCIS to forced torsional vibration of multiple-DOF systems, studying the properties of initializations by numerical simulation. We studied wave propagation properties in a multiple-DOF periodic system theoretically to obtain optimal parameters for the imaginary system, conducting experiments to verify the effectiveness of WCIS.

2. Control Law

2.1 Control strategy

The 1D torsional vibration system considered consists of torsional bars and rigid discs (Fig. 1). Rigid lines represent the real system and dotted lines the imaginary system. Our control is to compensate for torque, i.e., generated at the imaginary connecting torsional bar between the real and imaginary discs, $k_{m+1}\phi_{m+1}$, by an actuator, and to absorb vibration energy in the real system propagated to the imaginary system. The imaginary system is assumed to have sufficient DOF. This process involves a quasi-infinite system and realizes nearly steady-state wave propagation. The procedure is explained as follows by the use of the equation of motion:

Consider an (m+n)-DOF torsional vibration system in which the controlled real system is m-DOF and the imaginary system n-DOF. If only T_0 as disturbance torque, is applied to the left end disc of the real system, The equation of motion is expressed as

$$\ddot{\phi}_1 + \frac{k_1}{I_{0,1}}\phi_1 - \frac{k_2}{I_1} = -\frac{T_0}{I_0} \quad \cdots$$

$$\ddot{\phi}_m - \frac{k_{m-1}}{I_{m-1}}\phi_{m-1} + \frac{k_m}{I_{m-1,m}}\phi_m - \underline{\frac{k_{m+1}}{I_m}\phi_{m+1}} = 0$$

$$\ddot{\phi}_{m+1} - \underline{\frac{k_m}{I_m}\phi_m} + \frac{k_{m+1}}{I_{m,m+1}}\phi_{m+1} - \frac{k_{m+2}}{I_{m+1}}\phi_{m+2} = 0$$

$$\cdots$$

$$\ddot{\phi}_{m+n} - \frac{k_{m+n-1}}{I_{m+n-1}}\phi_{m+n-1} + \frac{k_{m+n}}{I_{m+n-1,m+n}}\phi_{m+n} = 0$$

$$I_{i,j}^{-1} \equiv I_i^{-1} + I_j^{-1} \qquad (1)$$

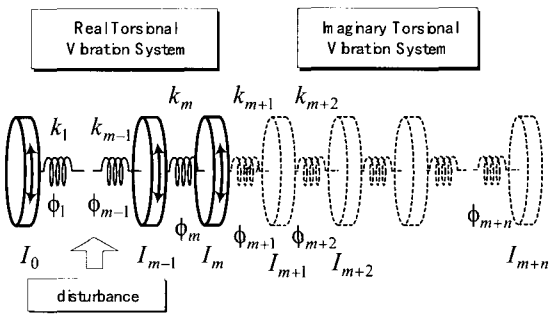

Fig. 1 Real and imaginary torsional vibration systems connected

where k_i, I_i, ϕ_i are the spring constant of i-th torsional bar, the moment of inertia of i-th rigid disc, and the torsional angle of i-th torsional bar, respectively. External disturbance on the i-th disc is expressed as T_i. The moment of inertia of the left-end disc and the external disturbance on it are represented by I_0 and T_0.

The vibration energy in the real system propagates to the imaginary system based on propagation properties when Eq. (1) is completely realized. Elements whose suffixes exceed (m+1) in Eq. (1) are virtual, so we must compensate for the term relating to ϕ_{m+1} (underlined in Eq. (1)) as control acceleration. Equations of motion including variables whose suffixes exceed (m+1) are solved by online calculation, where variable ϕ_m (underlined in Eq. (1)) is measured. This process is a feedforward control with single input and single output because the measured variable ϕ_m is not compensated for directly.

The above control strategy is based on the concept that wave-absorption control is equivalent to making the controlled system having no wave reflections at the boundary, i.e., to virtually realize an infinite structure in a finite structure. Our control strategy to connect a virtually large DOF system with initialization detailed in the section below is wave-absorption control, even though the control strategy does not use wave absorption conditions as in wave control of elastic continuous structures.

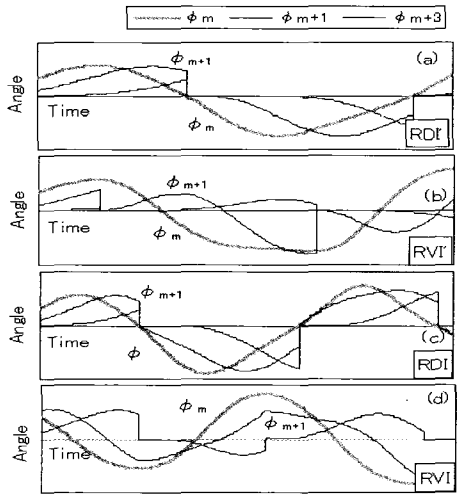

Fig. 2 Initialization of R-type for m-DOF real and n-DOF imaginary systems

(a) RDI': $\phi_{m+i} = \dot{\phi}_{m+i} = 0$ (i=1 to n) at $\phi_m = 0$,

(b) RVI': $\phi_{m+i} = \dot{\phi}_{m+i} = 0$ (i=1 to n) at $\dot{\phi}_m = 0$,

(c) RDI: $\phi_{m+i} = \phi_{m+1} = \dot{\phi}_{m+i} = 0$ (i=2 to n) at $\phi_m = 0$,

(d) RVI: $\phi_{m+i} = \phi_{m+1} = \dot{\phi}_{m+i} = 0$ (i=2 to n) at $\dot{\phi}_m = 0$

2.2 Initialization of imaginary systems

In an insufficient-DOF imaginary system for total energy to be absorbed, the imaginary system must have no kinetic or potential energy, with initialization of the imaginary system at appropriate timing. We use the following initialization (Saigo et al., 1998); when $\phi_m=0$ or $\dot{\phi}_m=0$, all imaginary variables are set to zero, $\phi_{m+i}=\dot{\phi}_{m+i}=0$ (i=1 to n), which we term RDI' and RVI'. These initializing timings are considered to influence the real system less because no energy or energy flow exists in connecting spring k_m at this moment. The continuity of $\dot{\phi}_{m+1}$ in RDI' and ϕ_{m+1} in RVI' may enhance control performance, termed RDI and RVI, RDI sets $\phi_{m+1}=\phi_{m+i}=\dot{\phi}_{m+i}=0$ (i=2 to n) when $\phi_m=0$ and keeps $\dot{\phi}_{m+1}$ unchanged, and RVI sets $\phi_{m+i}=\dot{\phi}_{m+1}=\dot{\phi}_{m+i}=0$ (i=2 to n) when $\dot{\phi}_m=0$ and keeps ϕ_{m+1} unchanged. These are tried for the first time, to our knowledge, in this paper. The above 4 methods initializing at $\phi_m=0$ or $\dot{\phi}_m=0$, RDI', RVI', RDI and RVI (R-methods) are modified to IDI', IVI', IDI, and IVI (I-methods) initializing at $\phi_{m+1}=0$ or $\dot{\phi}_{m+1}=0$. R-methods are based on the vibration state of the real system and I-methods on the imaginary system. In diagrammed R-methods (Fig. 2), initialization is conducted at each timing of $\phi_m=0$ or $\dot{\phi}_m=0$. It is sufficient to initialize systems after condition $|\phi_{n+m}|\geq\varepsilon$ is satisfied, where positive ε is given appropriately. Reducing the number of initializations per unit time diminishes the undesirable influence of initialization on the real system, but it is difficult to get optimum ε theoretically because it depends on the vibration state of the system.

2.3 Optimization of imaginary system

To obtain optimal parameters of the imaginary system as a vibration energy absorber, we analyzed a periodic disc-and-torsional spring system theoretically. The k-th equation of motion of the system (Fig. 3) is

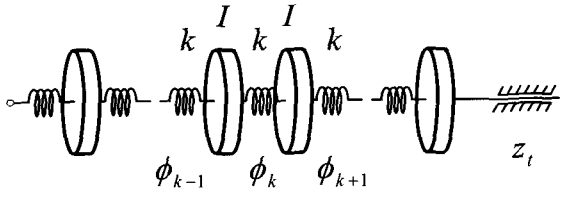

Fig. 3 Homogeneous disc and torsional spring system with terminal impedance

$$\ddot{\phi}_{k+1}-\omega_0{}^2\phi_k+2\,\omega_0{}^2\phi_{k+1}-\omega_0{}^2\phi_{k+2}=0 \tag{2}$$

where $\omega_0{}^2\equiv k/I$.

Laplace transformation of Eqn.(2) is

$$\Phi_{k+2}(s)-(2+\omega_0{}^2s^2)\Phi_{k+1}(s)+\Phi_k(s)=0 \tag{3}$$

where $\Phi_k(s)$ is Laplace transformation of $\phi_k(t)$.

Substituting general solution $\Phi_k(s)=\beta^k$ into Eq. (3), we obtain the specific roots

$$\begin{aligned}\beta&=1+s^2\omega_0^2/2\ \mp\sqrt{(1+s^2\omega_0^2/2)^2-1}\\&\equiv 1+s^2\omega_0^2/2\ \mp\sqrt{\beta^0}\ \equiv\ \beta^+,\beta^-\end{aligned} \tag{4}$$

and the general solution

$$\Phi_k(s)=c_1(s)(\beta^+)^k+c_2(s)(\beta^-)^k\equiv\Phi_k^+(s)+\Phi_k^-(s) \tag{5}$$

where $c_1(s)$ and $c_2(s)$ are arbitrary constants determined by boundary conditions.

When β^0 in Eq. (4) is negative, β^+ represents a positive propagating solution and β^- a negative propagating solution. By introducing $s=j\omega$ (j is the imaginary unit), the condition of existence of propagating solution $\beta^0\leq 0$ gives the limit frequency as

$$\omega\leq 2\omega_0 \tag{6}$$

The mechanical impedance for the positive propagating solution is

$$z^+(s)=\frac{s}{k(1-\beta^+)} \tag{7}$$

When terminal impedance z_t is $z^+(s)$, no wave reflection occurs.

The no wave reflection above is ideal as a wave absorber and expressed in mobility form as

$$\lambda=\frac{k}{\omega_0}\left\{\sqrt{1-\frac{1}{4}\left(\frac{\omega}{\omega_0}\right)^2}-j\frac{\omega}{2\omega_0}\right\} \tag{8}$$

Eq. (6) shows that the disc-and-torsional spring wave absorber must have a specific frequency i.e., $\omega_0=\sqrt{k/I}$ greater than half of the disturbance frequency of the controlled system. Eq. (8) shows that a larger spring constant better absorbs the vibration energy for a given input velocity and a specific frequency.

From Eq. (4), we obtain

$$|\beta^{+(-)}|^2=1 \tag{9}$$

which means the steady state wave amplitude is constant regardless of the frequency. The wave propagation condition thus realizes no resonance occurring in the standing-wave

condition, but antiresonance phenomena simultaneously disappear. The amplitude of the wave propagation condition near the frequency of antiresonance occurring in a standing-wave condition may exceed that of uncontrolled amplitude, although these amplitudes are very small.

The phase difference between two adjacent elements in a wave propagation condition is obtained by substituting $s=j\omega(=j\nu\omega_0)$ to β^+ of Eq. (4) (Fig. 4) where $\nu=\omega/\omega_0$. Eq. (9) and Fig. 4 evidence the wave propagation condition of a vibrating system.

3. Numerical Simulation

Here, we treat a 3-DOF real system where all torsional springs and discs are the same. Parameters of the analytical real system are the same as those of the experiment detailed in the next section, the moment of inertia $I=0.0123kgm^2$, and spring constant of torsional bar k=21.4 Nm. Parameters of the imaginary system are the same as for the real system except for the number of DOF. Disturbance torque T_0 is applied to the left end disc of the real system.

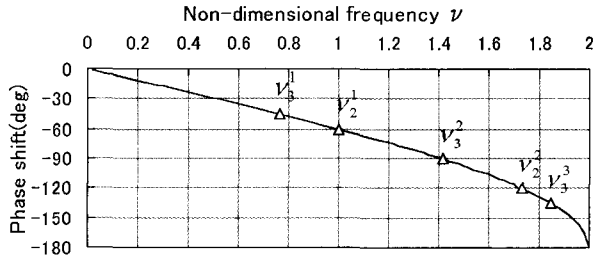

Fig. 4 Phase difference in torsional angle between adjacent elements. ν_i^j ; Nondimensional resonance frequency (i: number of DOF, j: number of mode; $\nu_2^1=1.0$, $\nu_2^2=1.73$, $\nu_3^1=0.765$, $\nu_3^2=1.41$, $\nu_3^3=1.85$,)

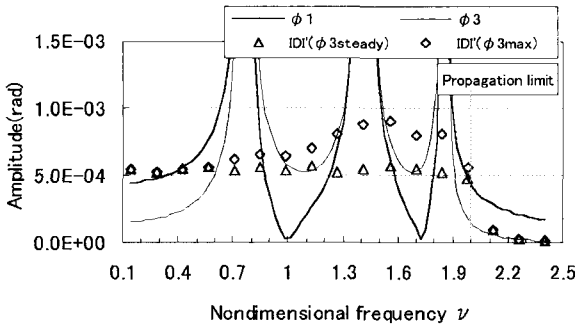

Fig. 5 Calculated response of 3-DOF real system to disturbance $\sin(\nu\omega_0 t)$ ($\omega_0=\sqrt{k/I}$; $\nu=0.566$) using 40-DOF imaginary system and IDI' initialization

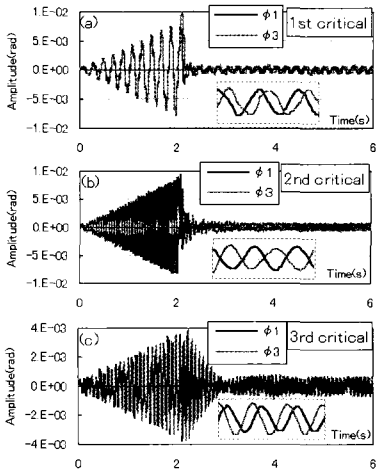

Fig. 6 Response by control starting 2 s of 3-DOF real system at resonance speeds with 40-DOF imaginary system and IVI initialization at (a) first resonance speed ν=0.765, (b) sencond resonance speed ν=1.41, and (c) third resonance speed ν=1.85.

Fig. 5 shows the controlled amplitude versus disturbance frequency with a 40-DOF imaginary system and IDI' initialization. △ denotes the steady-state amplitude in which the influence of initialization died away, and ◇ the maximum amplitude just after initialization. Steady-state amplitudes are constant below the wave propagation limit frequency given by Eq. (6), which coincides with the analytical result Eq. (9). These steady-state amplitudes coincide with a sufficiently large-DOF system obtained by modal vibration analysis with nearly zero frequency disturbance, not with those of a 3-DOF system.

Fig. 6 shows the timing chart at resonance frequencies. Control starts 2 seconds after disturbance is applied. These are typical features of wave control; after control starts, all amplitudes propagate with the same magnitude and constant phase shift through a transient period. We compare the phase difference in a wave propagation state between ϕ_1 and ϕ_3 (Fig. 6) and analytical states (Fig. 4). The theoretical phase shift between adjacent elements at frequencies $\nu=$ 0.765 (first resonance frequency), 1.41 (second resonance frequency) and 1.85 (third resonance frequency) are -45, -90 and -135 degrees. Note the phase difference between ϕ_1 and ϕ_3 (not ϕ_2) is about 2×(-45), 2×(-90) and 2×(-135) degrees, coinciding with the theoretical ones.

We have presented 8 types of initialization -- RDI, RDI', RVI, RVI', IDI, IDI', IVI, and IVI'. We found no general qualitative tendency among these methods by simulation, however, because controlled amplitudes depend on computation conditions such as initial conditions, ε detailed in Section 2.2, and the number of DOF of real and imaginary

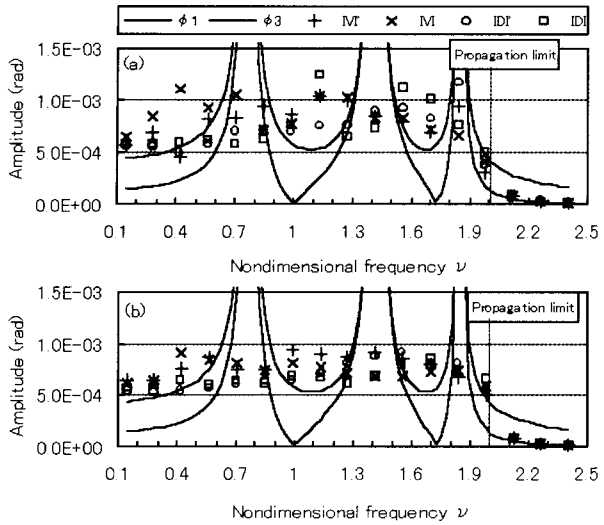

Fig. 7 Maximum response of ϕ_3 by wave control with (a) 10-DOF and (b) 40-DOF imaginary systems

systems. We cannot yet conclude which method is best. Below, we show results of I-methods as examples.

Fig. 7 shows maximum amplitudes versus disturbance frequency for 10-DOF and 40-DOF imaginary systems. Maximum amplitudes depend significantly on the disturbance frequency. Frequent initialization due to the smallness of the imaginary system does not give a steady-state condition. Initialization occurs before steady state vibration is established. It is not easy to theoretically determine the general tendency of initialization because amplitude just after initialization depends on the vibration state of the real system and initializing timing. Comparing Figures 7(a) and 7(b), the 40-DOF imaginary system shows better performance in initialization than the 10-DOF imaginary system, so the best way to avoid the undesirable influence of initialization is to use a large DOF imaginary system.

4. Experiment

Fig. 8 shows the experimental apparatus. The real vibration system consists of discs 200 mm in diameter and 20 mm thick and torsional bars 4 mm in diameter and 100 mm long for 2- and 3-DOF systems and 210 mm long for 1-DOF systems. AC servomotors are used for drive and control. The drive motor has a rated torque of 0.9 Nm and a rated speed of 3000 rpm and the control motor has a rated torque of 0.16 Nm and a rated speed of 3000 rpm. The measurement system consists of rotary encoders, a torsional angle converter, low-pass and high-pass filters, and a personal computer (CPU clock: 266 MHz). Torque disturbance is applied by torque fluctuation of the AC drive

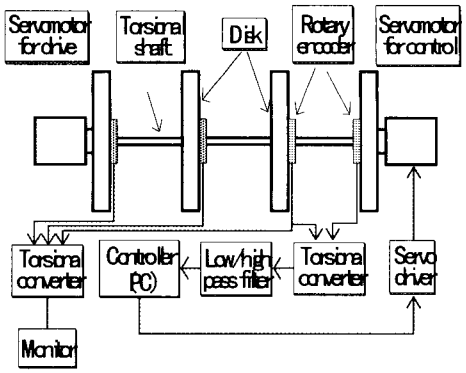

Fig. 8 Experimental apparatus

motor in constant speed mode, which is 4 times, 2 times, and 1 time per rotation, so resonance may occur at a rotation speed of 1/4, 1/2, and 1/1 of the natural frequency. Torque magnitude cannot be adjusted. A 10-DOF imaginary system is computed by the Euler method with a sampling period of 3 ms. Experiments are conducted for 1 DOF, 2 DOF, and 3 DOF.

Fig. 9 shows controlled and uncontrolled amplitudes at the first resonance frequency of the 2-DOF real system, where control starts at about 0.8 sec. Fig. 9(a) shows amplitudes of ϕ_1 and ϕ_2. Figures 9(b) and 9(c) show ϕ_1 and $2\phi_2$ on the magnified time scale. Amplitudes are suppressed considerably by control and the phase between ϕ_1 and ϕ_2 of the controlled amplitudes is shifted. The nondimensional frequency of the first torsional resonance of the 2-DOF real system ν_2^1 is 1, and the corresponding theoretical phase shift is -60 degrees (Fig. 4).

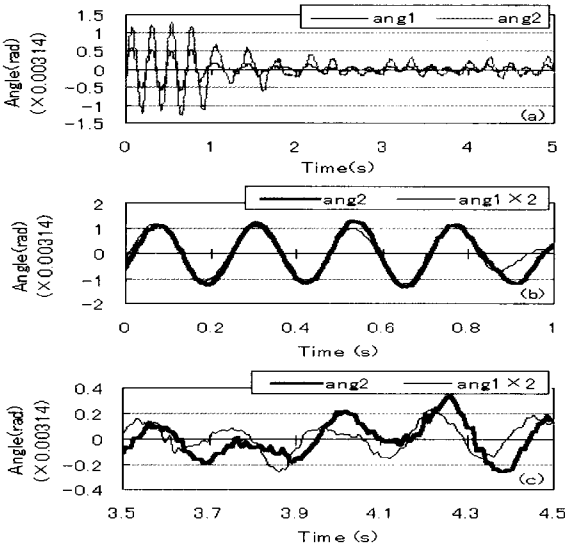

Fig. 9 Experimental waveforms of 2-DOF real system at 4.32 Hz excitation (first mode resonance frequency); ang1: ϕ_1, ang2: ϕ_2

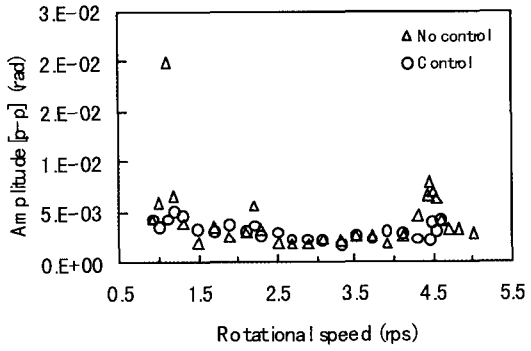

Fig. 10 Experimental response of 1-DOF real system

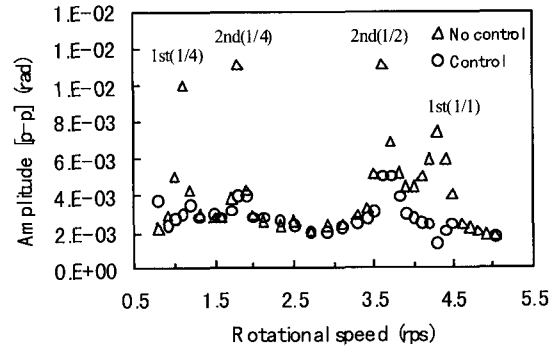

Fig. 11 Experimental response of 2-DOF real system

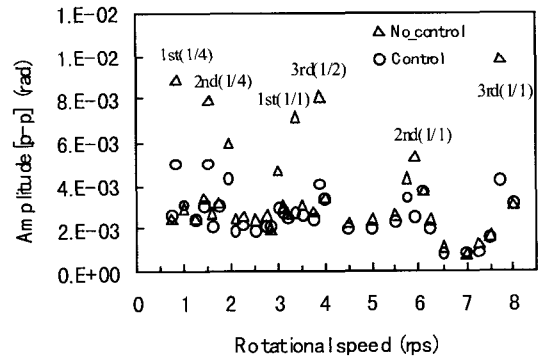

Fig. 12 Experimental response of 3-DOF real system

Fig. 9(c) shows the phase difference between ϕ_1 and ϕ_2 is about -60 degrees. The correspondence of phase shifts between experimental and theoretical results shows that wave control is realized in the experimental setup.

Fig. 10 shows experimental results for the 1-DOF real system with RDI' initialization. Resonance occurs at 1.1 rps, 2.2 rps, and 4.4 rps when uncontrolled, and the effect of vibration suppression by control is marked at these resonance speeds. Fig. 11 shows experimental results for the 2-DOF real system with RDI' initialization. Resonance occurs at 0.92 rps and 4.3 rps of the first mode resonance, and 1.81 rps and 3.62 rps of the second mode resonance when uncontrolled. At these resonance speeds, vibration amplitudes are markedly suppressed by control. Fig. 12 shows experimental results for the 3-DOF real system with RVI' initialization. Resonance occurs at 0.84 rps and 3.37 rps of the first mode resonance, 1.48 rps and 5.9 rps of the second mode resonance, and 3.86 rps and 7.72 rps of the third mode resonance. Though control effect is somewhat worse than for 1-DOF and 2-DOF systems, vibration amplitudes are suppressed in this case, also.

The present experimental apparatus is not perfect for WCIS, but experimental results show that it is possible to realize easily wave-absorption control with an imaginary system for forced vibration.

5. Conclusions

In this paper, we have investigated the effectiveness of wave-absorption control in suppressing torsional forced vibration, by simulation and experiment. Wave absorption control is possible in a 1D multiple-DOF torsional forced vibration system by connecting the imaginary and real systems and compensating for connection torque. And we have found that a larger DOF imaginary system reduces undesirable effects of initialization more than a smaller DOF imaginary system. The basic idea of this control method is easily applicable to any vibrating system even if only information on the structure where waves propagate is known. This control can be applied in many engineering fields through further work.

References

Brillouin, L. (1953). Wave Propagation in Periodic Structures, Dover Publications.

Elliott, S.J. and Billet, L. (1993). "Adaptive Control of Flexural Waves Propagating in a Beam", Journal of Sound and Vibration, Vol 163-2, pp 295-310.

Fujii, H., Ohtsuka, T. and Murayama, T. (1992a). "Wave Absorbing Control for Flexible Structures with Noncollocated Sensors and Actuators", J. Guidance, Control and Dynamics, Vol 15-2, pp 431-439.

Fujii, H. and Ohtsuka, T. (1992b). "Experiment of a Noncollocated Controller for Wave Cancellation", AIAA J. Guidance, Control and Dynamics, Vol 15-3, pp 741-745.

Gardonio, P. and Elliott, S.J. (1996). "Active Control of Waves on a One-dimensional Structure with a Scattering Termination", Journal of Sound and Vibration, Vol 192-3, pp 701-730.

Matsuda, K., Kanemitsu, Y. and Kijimoto, S. (1998). "A

Wave-based Controller Design for General Flexible Structures", Journal of Sound and Vibration, Vol 216-2, pp 269-279.

Miller, D.W. and von Flotow, A.H. (1989). "A Travelling Wave Approach to Power Flow in Structural networks", J. Sound & Vibration, Vol 128, pp 145-162.

O'Connor, W. and Lang, D. (1998). "Position Control of Flexible Robot Arms Using Mechanical Waves", ASME J. Dynamic Systems, Measurement and Control, Vol 120, pp 334-339.

Saigo, M., Tanaka, N. and Tani, K. (1998). "An Approach to Vibration Control of Multiple-Pendulum System by Wave Absorption", ASME J. Vibration and Acoustics, Vol 120, pp 524-533.

Utsumi, M. (1999). "Analytical Implementation of Wave-Absorbing Control for Flexible Beams Using Synchronization Condition", ASME J. Vibration and Acoustics, Vol 121, pp 468-475.

Von Flotow, A.H. (1986a). "Traveling Wave Control for Large Spacecraft Structures", AIAA J. Guidance, Control and Dynamics, Vol 9, pp 462-468.

Von Flotow, A.H. (1986b). "Disturbance Propagation in Structural Networks", J. Sound & Vibration, Vol 106, pp 433-450.

2002년 12월 6일 원고 접수
2003년 1월 17일 최종 수정본 채택